EVIDENCE OF DISCREPANCIES BETWEEN COLUMNAR-AVERAGED LIDAR RATIOS MEASURED BY SUN PHOTOMETER AND LIDAR BY MEANS OF A RAMAN LIDAR IN BARCELONA

Michaël Sicard[(1)], Francesc Rocadenbosch[(1)], Aurélien Hénon[(2)], Carlos Pérez[(3)], Alejandro Rodríguez[(1)], Constantino Muñoz[(1)], David García Vizcaino[(1)], Adolfo Comerón[(1)], Jose Maria Baldasano[(2, 3)]

[(1)] UPC, TSC, c/ Jordi Girona, 1-3, 08034 Barcelona (Spain), E-mail: msicard@tsc.upc.edu
[(2)] UPC, LMA, Avda Diagonal, 647, 08028 Barcelona (Spain)
[(3)] BSC, c/ Jordi Girona, 29, 08034 Barcelona (Spain)

ABSTRACT

Sun photometer and backscatter lidar measurements of a diurnal cycle are analyzed in terms of aerosol optical thickness (AOT), size distribution, single scattering albedo (SSA) and extinction-to-backscatter ratio (lidar ratio) in Barcelona, Spain. An a posteriori measurement of the lidar ratio profile has been made possible thanks to the first Raman lidar measurement in Barcelona. In most part of the atmospheric boundary layer (ABL), the columnar-averaged lidar ratio is well estimated by the sun photometer but it is underestimated by the elastic lidar. The possibility that this latter disagreement be explained by combined increase of relative humidity and aerosol absorption with the vertical variability of the size distribution is being studied. A mean lidar ratio of 50 sr is found in the ABL, and a thin layer of aerosols with lidar ratios of about 80 sr is detected at its top.

1. INTRODUCTION

Backscatter lidar has proven to be an effective instrument for obtaining high-resolution profiles of atmospheric aerosols' optical coefficients. However the solution of the backscatter lidar equation requires accurate system calibration and assumptions regarding the aerosol lidar ratio [1][2].

Many authors have used a combination of backscatter lidar measurements and sun photometer AOT measurements to obtain the columnar-averaged values of the lidar ratio [3][4][5]. This method gives a good estimation of the columnar-averaged lidar ratio when the aerosols' optical properties are homogeneous in both the horizontal and vertical directions, like e.g. in cases such as over great plains or long-range transport. In [5] an uncertainty on the lidar ratio as good as ± 8 % was found.

In Barcelona, we frequently experience multi-layered aerosol structures. This paper is focused on the evaluation of the commonly-used forcing of the lidar inversion with sun photometer AOT by means of a Raman lidar.

2. SUMMARY OF INSTRUMENTS AND OBSERVATIONS

2.1 The UPC Scanning Raman Lidar

A transportable, steereable lidar system allowing three-dimensional scans has been developed at the Universitat Politècnica de Catalunya (UPC) [6]. A Raman channel has been successfully added to the system and a beta version of the automated variable-resolution algorithm described in [7] is in use. The present system is based on an Nd:YAG laser working at the 1064-nm fundamental wavelength and at the 532-nm second harmonic, delivering pulses at 20 Hz of equal energy (160 mJ) and 6-ns duration. A 20-cm diameter telescope collects the backscattered light. Two avalanche photodiodes (APDs) detect the signals at the laser wavelengths and a photomultiplier tube (PMT) is used for the Raman scattered light from the nitrogen molecules at 607.4 nm. At the time the measurements were taken, the detectors were placed alternatively at the telescope output. The emission and reception axes are different so that a blind zone is observed between 0 and 200 m. However, the overlap factor reaches 1 rapidly, and is full within less than 400 m.

2.2 Microphysical analysis from sun photometer measurements

AOT measurements were taken using a CIMEL multi-wavelength sun-photometer, part of the global-scale Aerosol Robotic Network (AERONET)[8]. Size distribution, SSA and phase function measurements from the sun photometer are also used in this paper. In all cases, the Angström exponent (AE) which describes the spectral dependence of all these quantities was calculated with the AOTs at 440 and 670 nm. It was then used to estimate each measured quantity at the laser wavelength of 532 nm by correcting the quantities from the 440-nm channel.

The column-averaged lidar ratio, $S_S(\lambda)$, can be calculated from the SSA, $w(\lambda)$, and the particle phase function at 180º, $P(\lambda,180º)$:

$$S_S(\lambda) = \frac{4\pi}{w(\lambda)P(\lambda,180^o)} \qquad (1)$$

As on both days the size distribution is dominated by small particles in more than half of the measurements (with radii < 1 μm, see Fig. 5d and 5e), the calculation of the SSA and the phase function is made with the almucantar retrieval model for spherical particles.

2.3 Observations

Two days of measurements made in Barcelona (41º23' N 2º07' E, 115 m asl) are explored:
- a full diurnal cycle of lidar measurements at 532 nm on February 18th, 2005 (18Feb05). Fig. 1 shows the square range-corrected lidar signal as a function of time and altitude. The ABL height is approximately constant throughout the day at about 500 m, then starts to increase at 16UTC, and reaches 800 m at 18UTC. Both sun photometer and lidar measurement times are completely overlapped.

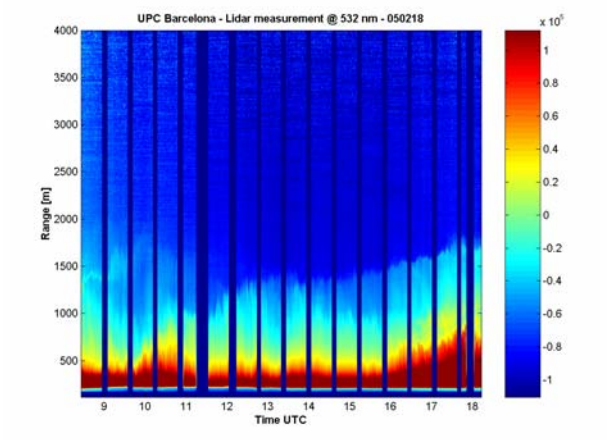

Fig. 1. 2D lidar cross-section of the backscattered lidar signal (arbitrary unit) at 532 nm as a function of time and altitude on 18Feb05.

The synoptic situation on 18Feb05 is depicted in Fig. 2 (left). It was characterized by an anticyclone over the north Atlantic Ocean and a strong low-pressure area over Scandinavia. The Iberian Peninsula (IP) is south of these two phenomena. Northern flows affected the study area during the whole day.

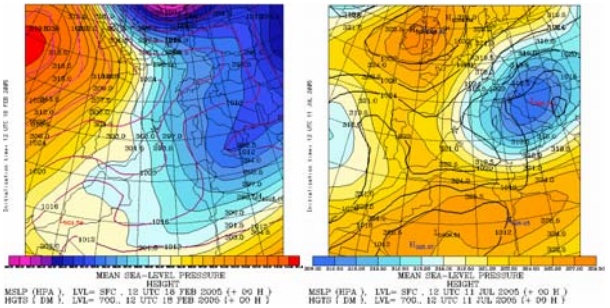

Fig. 2. Geopotential height at 700 hPa and MSL pressure on (left) 18Feb05, and (right) 11Jul05.

- a nighttime Raman lidar measurement at 532 and 607.4 nm on July 11th, 2005 (11Jul05). During daytime, only sun photometer data are available. The synoptic situation depicted in Fig. 2 (right) shows a weak pressure gradient at surface levels over the IP and the development of the Iberian Thermal low as an extension of the North African thermal low. The IP was surrounded by two low-pressure areas over the Atlantic Ocean and Central Europe. Northern flows affected the study area during the whole day. According to [9], the ABL expansion is expected to be very similar (maybe slightly higher) than on 18Feb05 since the same meteorological conditions are gathered.

The 4-day back trajectories computed by the Hysplit model from NOAA Air Resources Laboratory arriving in Barcelona at 500, 1500 and 2500 m are shown in Fig. 3. They confirm the general wind direction on both days from north to south and the continental origin of the air masses.

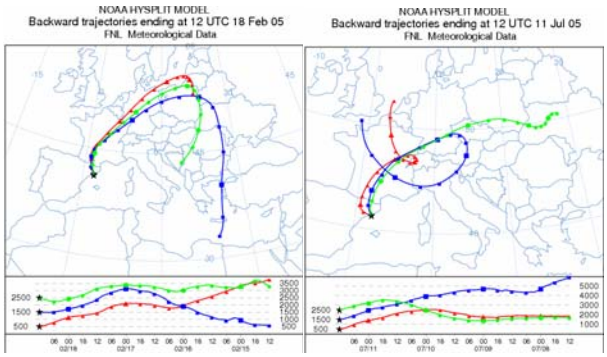

Fig. 3. 4-day Hysplit back trajectories arriving in Barcelona on (left) 18Feb05, and (right) 11Jul05.

According to the SeaWIFS satellite images, no Saharan dust was present on neither of these two days.

On 11Jul05 no diurnal cycle of lidar measurements is available. As the size of our collecting telescope does not allow daytime measurements of Raman signals (as opposed to the fact that sun photometer measurements can only be made during daytime), there is no other way than to assume the atmosphere stable between the last sun photometer measurements and the Raman lidar measurement.

3. RESULTS AND DISCUSSION

The behavior of the AOT is very similar on both days (Fig. 5a and 5b): it is slowly increasing along the day but stays relatively weak (< 03). The mean AE is around 1.8 and has also the same behavior on both days: it reaches a very slight minimum between 12 and 14UTC. The small variability of the AOT between

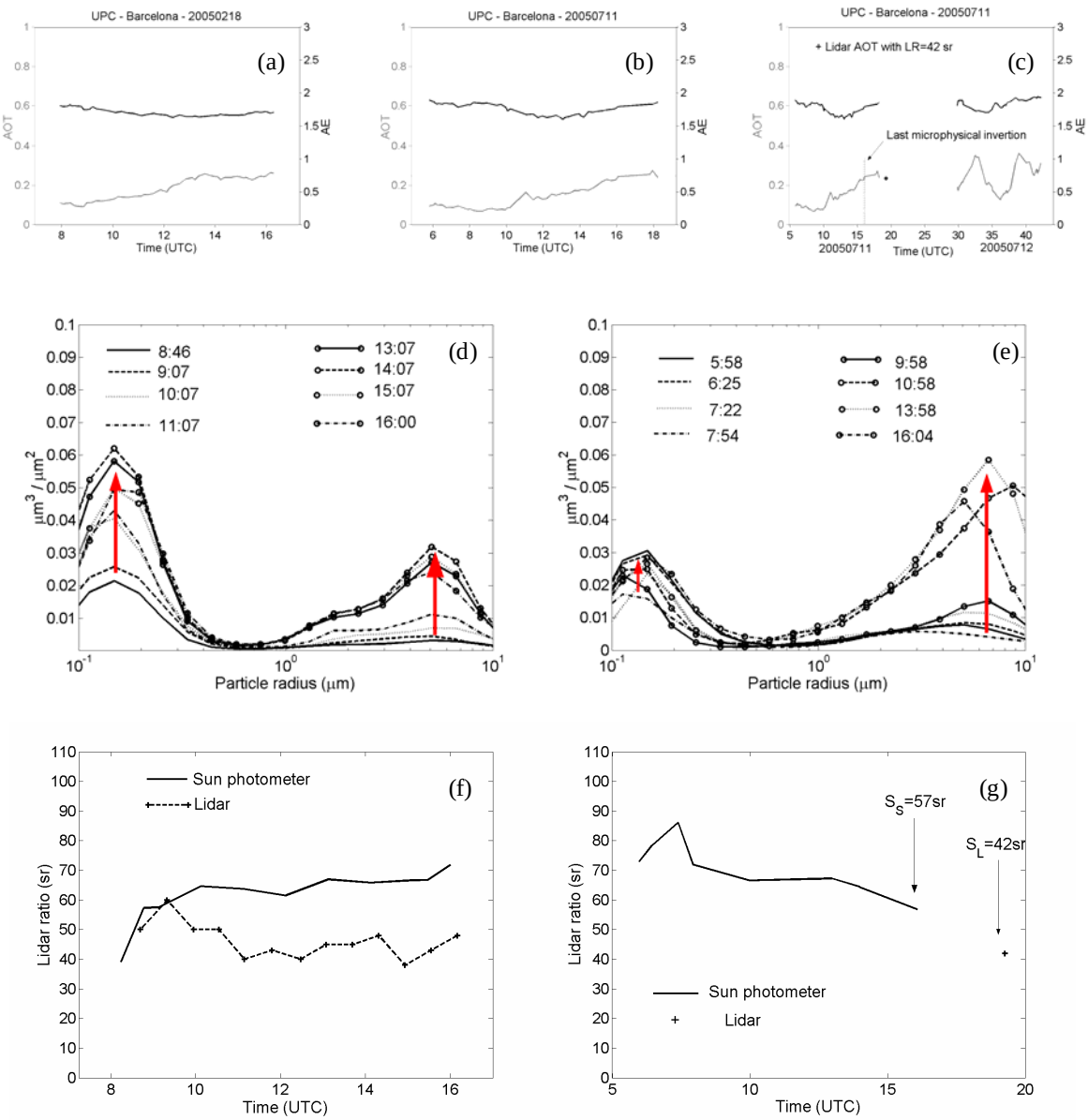

Fig. 5. Sun photometer AOT and AE at 532 nm on (a) 18Feb05, (b) 11Jul05, and (c) 11-12 July 2005. Volume size distribution on (d) 18Feb05, and (e) 11Jul05. Columnar-averaged lidar ratios on (f) 18Feb05, and (g) 11Jul05.

11Jul05 and the following day can be checked in Fig. 5c where the AOT on both days is represented. AOT changes during nighttime are very weak.

On 18Feb05, the size distribution (Fig. 5d) shows two modes: a fine and a coarse mode centered on 0.15 μm and 5 μm, respectively. On 11Jul05 (Fig. 5e), the size distribution is also bi-modal with a fine mode and a coarse mode centered on 0.14 and 6 μm, respectively. The size distributions at the beginning of both days are very similar with a dominant fine mode. As the day goes by, the proportion of both modes increases moderately in equal proportions on 18Feb05 (and the fine mode end up being dominant), whereas the proportion of the fine mode weakly increases and the proportion of the coarse mode strongly increases on 11Jul05 (so that at the end the coarse mode is the dominant one).

The weak AOTs and the relatively large contribution of the fine mode of the size distributions let think that anthropogenic aerosol coming from the lower layers of the atmosphere may be the main constituent of the ABL.

In the elastic lidar inversion procedure, the value of the lidar ratio, S_L, is adjusted until the AOT retrieved by integrating the lidar extinction coefficient profile equals the sun photometer AOT. The slight increase of S_S (Fig. 5f), while the AOT increases and the SSA decreases (not shown), is due to the increase of

absorption and extinction of small particles [3]. However the behavior of S_L is opposite to that of S_S: it slightly decreases, and in the second half of the day the difference between both lidar ratios is about 20 sr. This large difference is probably indicating large variations in aerosol physical properties with altitude.

On 11Jul05, S_L and S_S are compared to the Raman-inverted lidar ratio (Fig. 5g and 6). The statistical error due to the signal detection is the main source of error considered for the calculation of the errorbars enveloping the solid curve. The lidar ratio profile indicates a linear decrease from 400 up to 1000 m and a strong increase to about 80 sr in the [1; 1.5 km] region. The combined increase of the absorption and the relative humidity at the top of the ABL may explain the lidar ratio vertical variability [10]. A change of the size distribution in the [1; 1.5 km] region might be an additional explanation to this phenomenon. These results suggest the presence of rather large anthropogenic aerosols in the ABL.

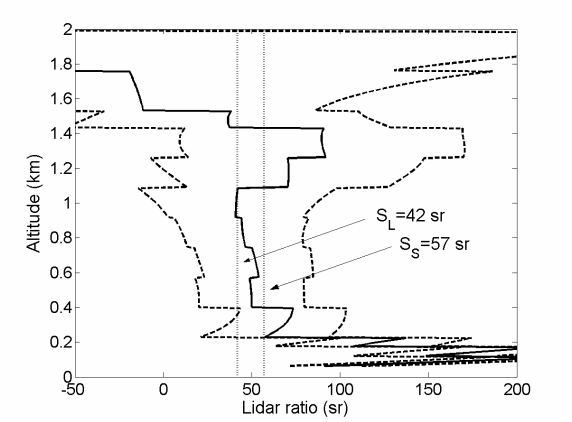

Fig. 6 Inverted Raman lidar ratio on 11Jul05 (the error bars are represented by the dashed curves).

4. CONCLUSION

In the two cases presented, columnar-averaged lidar ratio from sun photometer measurement appears to be a good integrated value of the lidar ratio, whereas S_L has a tendency to underestimate the columnar-averaged value. An averaged value of S_S of 50 sr is found in the ABL, but a large jump up to 80 sr is observed at its top. In such cases, any attempt to estimate the aerosol extinction profile by forcing the lidar inversion with the sun photometer AOT may lead to significant errors. In Barcelona, the atmospheric structure reveals very often multiple layers [9], and in most cases forcing the lidar inversion with the sun photometer AOT leads to wrong optical coefficient retrievals. A Raman lidar is an essential tool to cope with this problem.

Acknowledgments. This work was supported by the EARLINET project from the European Commission under the grant EVR1-CT1999-40003 and by the CICYT (Spanish Interministry Commission of Science and Technology) project CICYT REN2003-09753-C02. The authors gratefully acknowledge the NOAA Air Resources Laboratory (ARL) for the provision of READY website (http://www.arl.noaa.gov/ready.html) and the HYSPLIT trajectory model. The Spanish Ministry of Science and Education is also thanked for the Ramón y Cajal position hold by M. Sicard.

References

1. Klett J. D.,. Stable analytical inversion solution for processing lidar returns, *Appl. Opt.*, Vol. 20, 211 – 220, 1981.

2. Fernald F. G.,. Analysis of atmospheric lidar observations: some comments, *Appl. Opt.*, Vol. 23, 652 – 653, 1984.

3. Takamura T., et al., Tropospheric aerosol optical properties derived from lidar, sun photometer, and optical particle counter measurements, *Appl. Opt.*, 33, 7132 – 7141, 1994.

4. Hayasaka T., et al., Optical Properties and Size Distribution of Aerosols Derived from Simultaneous Measurements with Lidar, a Sunphotometer, and an Aureolemeter, *Appl. Opt.*, 38, 1630 – 1635, 1999.

5. Pelon J., et al., Characterization of aerosol spatial distribution and optical properties over the Indian Ocean from airborne LIDAR and radiometry during INDOEX'99, *J. Geophys. Research*, 107, 8029 – 8041, 2002.

6. Rocadenbosch F., et al., The UPC scanning Raman lidar: an engineering overview, *Proc. of the 21st International Laser Radar Conference*, Vol. 1, 69 – 70, 2002.

7. Rocadenbosch F., et al., Automated variable-resolution algorithm for Raman extinction retrieval, *Proc. of the 22nd International Laser Radar Conference*, Vol. 1, 467 – 470, 2004.

8. Holben et al., AERONET – A federated instrument network and data archive for aerosol characterization, *Remote Sens. Env.*, 66, 1 – 16, 1998.

9. Sicard M., et al., Mixed-layer depth determination in the Barcelona coastal area from regular lidar measurements: methods, results and limitations, *Boundary-Layer Metorol.*, in press, 2006.

10. Ferrare R. A., et al., Raman lidar measurements of the aerosol extinction-to-backscatter ratio over the Southern Great Plains, *J. Geophys. Research*, 106, 20333 – 20347, 2001.